Strategy for Kinetic Parameter Estimation—Thermal Degradation of Polyurethane Elastomers

Ante Agić, Emi Govorčin Bajsić

Faculty of Chemical Engineering and Technology, University of Zagreb, 10 000 Zagreb, Croatia

Received 17 December 2005; accepted 3 June 2006
DOI 10.1002/app.25040
Published online in Wiley InterScience (www.interscience.wiley.com).

ABSTRACT: The kinetics of the thermal degradation of polyurethane (PU) elastomers based on poly(ether polyol) soft segments and an aromatic type of diisocyanate were investigated by thermogravimetric analysis (TGA) under a nitrogen atmosphere employing four heating rates. The corresponding kinetic parameters of the two degradation stages were estimated by minimizing the output error functional and by the Kissinger method. In evaluating the kinetic parameters of the two-step PU thermal decomposition, a differential thermogravimetry curve was applied as an objective functional in a regression procedure. Parameter estimation was obtained by minimizing the weighted quadratic output error functional with the modified Nelder–Mead simplex search algorithm. The confidence regions in the pre-exponential factor-activation energy space were established for both the first and second stages of degradation. The effect of the molecular weight of the soft segment and the content of the hard segment on the activation energy of the degradation process was constructed by response surface methodology. © 2006 Wiley Periodicals, Inc. J Appl Polym Sci 103: 764–772, 2007

Key words: polyurethane; degradation kinetics; modeling; thermogravimetric analysis (TGA)

INTRODUCTION

Thermal degradation of elastomeric polyurethane (PU) is of great importance in the development of a rational processing technology and extreme temperature durability. Computational modeling and simulation of degradative processes are essential for understanding many phenomena, such as chemical kinetic mechanisms, the influence of polymer morphology, and the effects of stabilizers and additives.[1] The PU materials must have brilliant mechanical properties over a wide temperature range with adequate resistance to the most degradative environment. The design of a temperature-resistant structure would be greatly improved through the development of a computational model, which could incorporate known quantities such as material microstructure, temperature, and chemical environment, from which descriptors such as the degraded state of the material in terms of exposure time and position in the structure could be determined. Polyurethane chains consist of alternating short sequences that form soft and hard segments as shown by Figure 1. The soft segment (SS), which originates in the polyol, imparts elastomeric characteristics to the polymer.[2] The hard segment (HS) act as a physical crosslink, and as a consequence, the physical and mechanical properties depend strongly on the degree of phase separation between the hard and soft segments and the interconnectivity of hard domains. Soft segments mainly consist of polyethers or polyesters, whereas the HS is composed of diisocyanate and the so-called chain extender, a low-molecular-weight diol. Microstructure parameters such as length of the HS, orientation and degree of crystallinity of the HS, molecular weight, and volume fraction of the polymer are primarily responsible for temperature durability and processability.

The observation of weight loss at elevated temperatures is a simple and very accurate way to study thermal degradation. Thermogravimetry (TGA) is a suitable method for evaluating the thermal properties of several types of polyurethane elastomers. These elastomers generally are not very thermally stable, especially above their softening temperatures, and their mechanism of thermal degradation is very complex because of the variety of products formed (see Fig. 2).

During a ramped heating under nitrogen, such as in a TGA experiment, the degradation process usually passes through three stages. In the first and second stages, the urethane bonds decompose to form alcohols and isocyanates. Complete volatilization of the resulting chain fragments is prevented by dimerization of the isocyanates to carbodiimides, which react with the alcohol groups to give relatively stable substituted ureas (second step) that decompose in the third stage. Trimerization of isocyanates may also occur under certain conditions to yield thermally stable isocyanurate rings. The final step is high-temperature

Correspondence to: Dr. Ante Agić (aagic@marie.fkit.hr).

Journal of Applied Polymer Science, Vol. 103, 764–772 (2007)

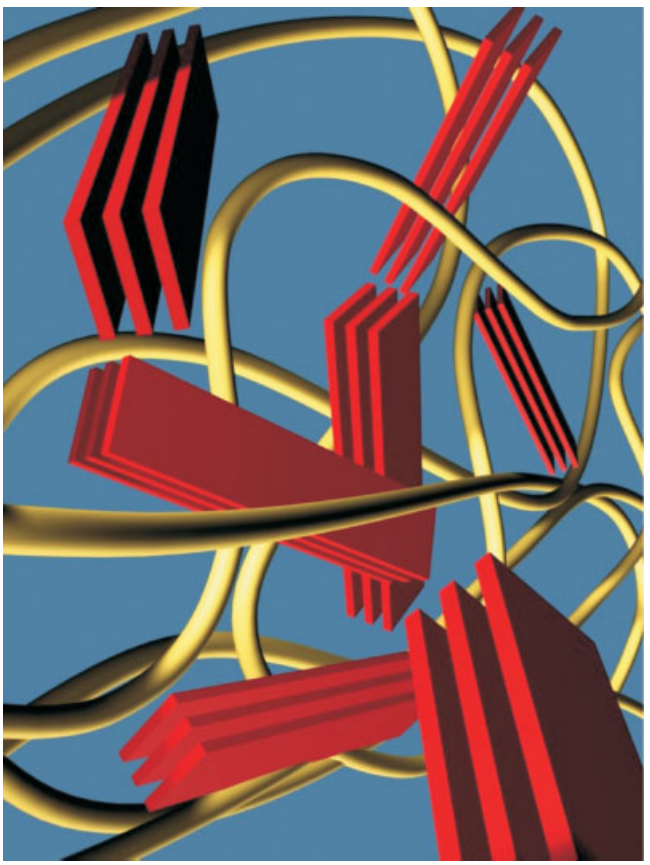

Figure 1 Structural model of PU elastomer. [Color figure can be viewed in the online issue, which is available at www.interscience.wiley.com.]

degradation of these stabilized structures in order to yield volatile products and a small quantity of carbonaceous char. It has been proposed that the thermal degradation of polyurethane is primarily a depolycondensation process that starts at about 250°C. Commonly, it presents a bimodal profile, with the first mode related to the HSs. Usually, at a low heating rate, the degradation process results in differential weight loss (DTG) curves with several peaks, which is an indication of the complexity of the degradation. Figure 3 illustrates the thermogravimetry (TG) and differential thermogravimetry curve for the PU elastomers based on poly(ether polyol) and aromatic diisocyanate at a heating rate of 10°C/min under nitrogen. The TG-DTG curve of the PU sample has two distinct regions of weight loss reflected in two peaks (maxima) in the DTG curve, implying that at least two stages of degradation occurred in this sample. The initial degradation, in the first stage, resulted primarily from the decomposition of the urethane HS segment, whereas the second stage proceeded by the depolycondensation and polyol degradation mechanisms and was affected by the SS content.[4–6]

The aim of this work was to develop a strategy for precise kinetic parameter estimation and confidence interval determination of thermal degradation of PU elastomers. The dependence of kinetic parameters on microstructural descriptors such as hard-segment content and soft-segment molecular weight was also established.

EXPERIMENTAL

Materials

Poly(oxytetramethylene glycol) (PTMO, molecular weights 1000 and 2000; BASF Co., Parsippany, NJ) formed the soft segment. The hard segment was composed of 4,4′-methylene bis(phenyl isocyanate) (MDI) from Mobay Chemical (Pittsburgh, PA) and the chain extender butane-1,4-diol (BD 1.4, Du Pont, Wilmington, DE).

Synthesis of PU elastomers

The PU elastomers were synthesized by a two-step procedure. First, the PU prepolymer was prepared at 80°C in a nitrogen atmosphere in a stirred-glass reaction kettle. MDI was placed into a reaction kettle equipped with a mechanical stirrer, reflux condenser, dropping funnel, and N_2 inlet and outlet, and the temperature was increased to 80°C. The appropriate amount of glycol was added dropwise to the reactor, NCO/OH molar ratios of 2 : 1 and 4 : 1. The reaction was continued until the NCO content reached the theoretical value as determined by dibutylamine titration.[6] A chain extender was added to the prepolymer under intensive mixing at a temperature of 90°C. After 60 s of mixing, the product was poured into a Teflon mold, and PU elastomers were prepared by hot-pressing in a Carver hydraulic press (Wabash, IN) at constant pressure. A temperature of 100°C for 30 min was used. The elastomers were postcured for 24 h at 105°C in an oven.

Characterization of material

Thermogravimetric analysis (TGA) was performed on a Du Pont 951 thermogravimetric analyzer (Du Pont, Wilmington, DE). The samples (7–10 mg) were heated from room temperature to 600°C at different heating rates (2°C/min, 5°C/min, 10°C/min, and 15°C/min) in nitrogen flowing at a rate of 60 mL/min.

Kinetic Model

It was assumed that the normalized mass change of a sample could be used as follows:

$$\frac{m - m_\infty}{m_0 - m_\infty} = \lambda_1 \cdot (1 - \alpha_1) + \lambda_2 \cdot (1 - \alpha_2) \qquad (1)$$

where m, m_0, and m_∞ are the actual, initial, and final masses, respectively; and α_1 and α_2 are the

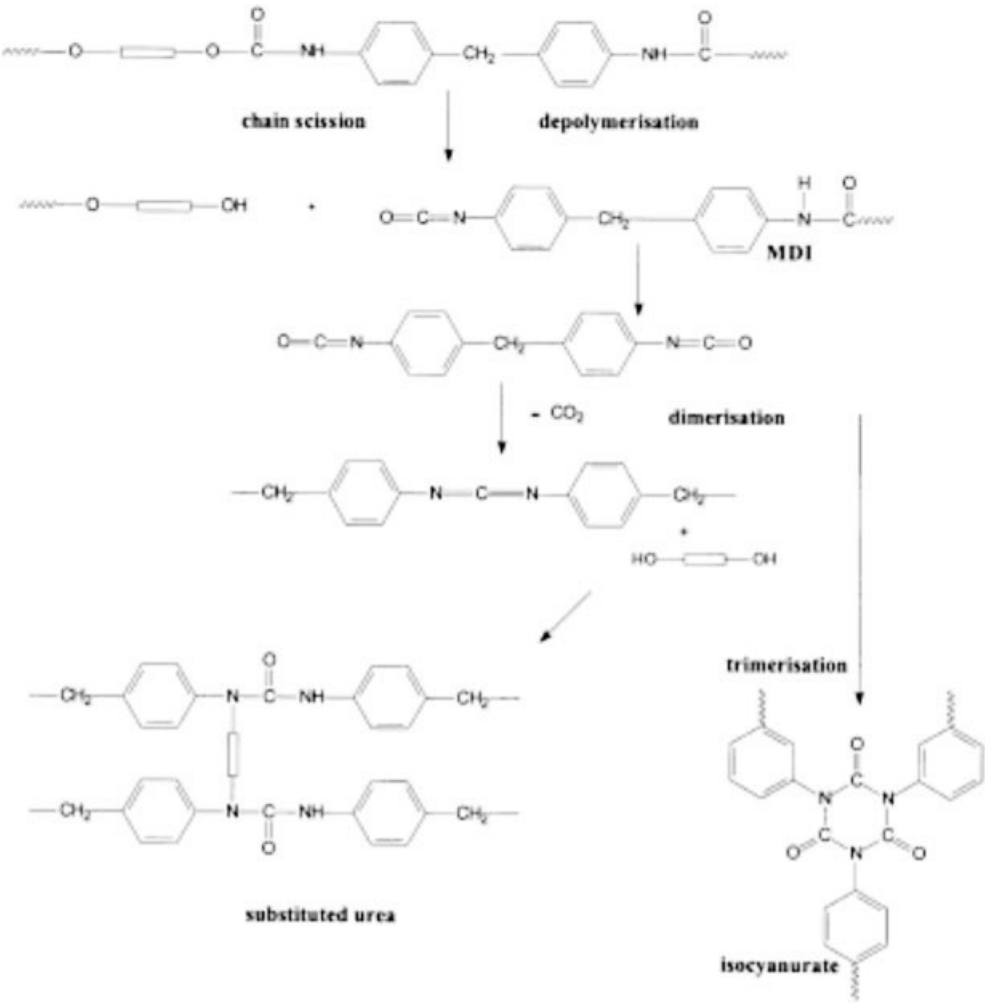

Figure 2 Mechanism of PU thermal degradation.

degrees of conversion of the first and second components, respectively. If degradation is conducted as a two-step process, the rate of conversion can be described by the following two ordinary differential equations[7]:

$$\frac{d\alpha_1}{dt} = A_1 \cdot \exp\left(-\frac{E_1}{RT}\right) \cdot f_1(\alpha_1)$$

$$\frac{d\alpha_2}{dt} = A_2 \cdot \exp\left(-\frac{E_2}{RT}\right) \cdot f_2(\alpha_2) \quad (2)$$

where $d\alpha_1/dt$ and $d\alpha_2/dt$ are the rates of degradation of the first and second components, respectively; A_i $i = 1, 2$ are the preexponential factors; E_1 and E_2 are the activation energies; R is the universal gas constant, T is the temperature; and f_i, $i = 1, 2$ are the conversion-dependent functions. Visual inspection of the thermal degradation curve (TG-DTG) allowed the assumption that each stage occurred independently [no coupling terms in eq. (2)].[8] If it were supposed that a TG-DTG curve was measured at a constant heating rate, $\beta = dT/dt$, upon integration the above equation could be rewritten in the form

$$\int_0^\alpha \frac{d\alpha}{f_1(\alpha)} = \frac{A_1}{\beta} \cdot \int_{T_0}^T \exp\left(-\frac{E_1}{RT}\right) dT$$

$$\int_0^\alpha \frac{d\alpha}{f_2(\alpha)} = \frac{A_2}{\beta} \cdot \int_{T_0}^T \exp\left(-\frac{E_2}{RT}\right) dT \quad (3)$$

where T_0 is the temperature at the beginning of degradation. The Arrhenius integral can be approximated by the following expansion[9]:

$$\int \exp\left(-\frac{E}{RT}\right) dT = \frac{E}{R} \exp(x) \frac{1}{x(x-2)} \times \left[1 + \frac{2}{x(x-2)} + \cdots\right] \quad (4)$$

where $x = -E/RT$. The degrees of conversion, $\hat{\alpha}_1$ and $\hat{\alpha}_2$, as analytical solutions of eq. (3) for the given

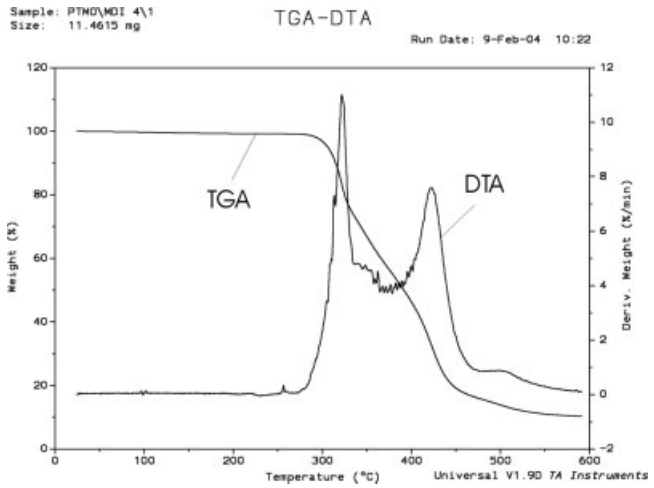

Figure 3 Two-step thermal degradation of PU.

conversion functions, $f_1(\alpha)$ and $f_2(\alpha)$, have the following forms:

$$\hat{\alpha}_1 = \Im_1\left(\frac{A_1}{\beta}, x, \xi\right)$$
$$\hat{\alpha}_2 = \Im_2\left(\frac{A_2}{\beta}, x, \zeta\right) \quad (5)$$

where ζ and ξ are the parameters that define the conversion functions. Therefore, the overall rate of conversion is given by the sum of the component rates of conversion:

$$\frac{d\alpha}{dt} = \lambda_1 \cdot A_1 \cdot \exp\left(-\frac{E_1}{RT}\right) \cdot f_1(\hat{\alpha}_1) + \lambda_2 \cdot A_2 \times \exp\left(-\frac{E_2}{RT}\right) \cdot f_2(\hat{\alpha}_2) \quad (6)$$

where λ_i is the yield coefficient of the ith weight loss stage, with constraints

$$\sum_{i=1}^{2} \lambda_i \leq 1 \quad (7)$$

The coefficient λ_i is associated with the level of separation of the stages of the TG curves. Many known kinetic models correspond with the mechanism of polymer degradation.[8] The proposed kinetic model should be based on fundamental chemical knowledge and not on the formal empirical model. Most research of polyurethane[2] has suggested that the rate of degradation is proportional to remaining amount of the component, with the following conversion functions:

$$f_1 = (1 - \alpha_1)^n$$
$$f_2 = (1 - \alpha_2)^m \quad (8)$$

where n and m are the reaction orders. The overall rate of conversion is given by the sum of the component rates of conversion with the following expression:

$$\frac{d\alpha}{dt} = \lambda_1 \cdot A_1 \cdot \exp\left(-\frac{E_1}{RT}\right) \times \left\{1 - (1-n)\frac{A_1}{\beta}\left[\frac{T}{(2-x)}\exp\left(-\frac{E_1}{RT}\right)\right]\right\}^{n/1-n} + \lambda_2 \cdot A_2 \cdot \exp\left(-\frac{E_2}{RT}\right) \times \left\{1 - (1-m)\frac{A_2}{\beta}\left[\frac{T}{(2-x)}\exp\left(-\frac{E_2}{RT}\right)\right]\right\}^{m/1-m} \quad (9)$$

The influence of the initial temperature, T_0, can be neglected. In case of the presence of the coupling term in the system of differential equations [eq. (2)], the equations can be solved numerically by integration procedures only. Recently, a nonparametric kinetics method was proposed[10] in order to overcome difficulties with choice of the proper conversion functions.

Parameter estimation and confidence region

The goal of kinetic parameter estimation is simply to determine the value of unknown parameters so that the modeled responses fit the measured outputs in the best possible ways. The unknown apparent kinetic parameters, that is, the ''kinetic triplets'' [preexponential factors (A_i), activation energies (E_i), and conversion functions (f_i)], of both reaction stages can be obtained by fitting the above kinetic equation [eq. (9)] to the experimental DTG curves. The kinetic parameters were determined by minimizing the weighted residual sum of squares of errors between the set of experimental observations, $(d\alpha/dt)|_{\text{exp}}$, and the corresponding set of model outputs, $(d\alpha/dt)|_{\text{calc}}$, as the measure of goodness of fit. For the given heating rate, β, the objective function should be rewritten as

$$\min_{\Theta,\beta} S(\Theta,\beta) = \sum_{i=1}^{N} \frac{1}{\sigma_i}\left(\frac{d\alpha}{dt}(T_i,\beta)\bigg|_{\text{exp}} - \frac{d\alpha}{dt}(T_i,\Theta,\beta)\bigg|_{\text{calc}}\right)^2 \quad (10)$$

subject to eq. (2) and $\sum_{i=1}^{2}\lambda_i \leq 1$ as constraints.

The vector $\Theta = \{A_1, E_1, \Xi, \lambda_1, A_2, E_2, \zeta, \lambda_2\}$ is the unknown-parameters vector, and σ_i is the weighting factor (variance), which attaches more or less importance to each point i. The variability in heating rate is overcome by the chosen reference objective function at the mean heating value, $\bar{\beta}$[8]

$$S(\Theta,\bar{\beta}) = \frac{1}{M}\sum_{k=1}^{M}\sum_{i=1}^{N}\frac{1}{\sigma_i} \times \left(\frac{d\alpha}{dt}(T_i,\beta_k)\bigg|_{\text{exp}} - \frac{d\alpha}{dt}(T_i,\Theta,\beta_k)\bigg|_{\text{calc}}\right)^2 \quad (11)$$

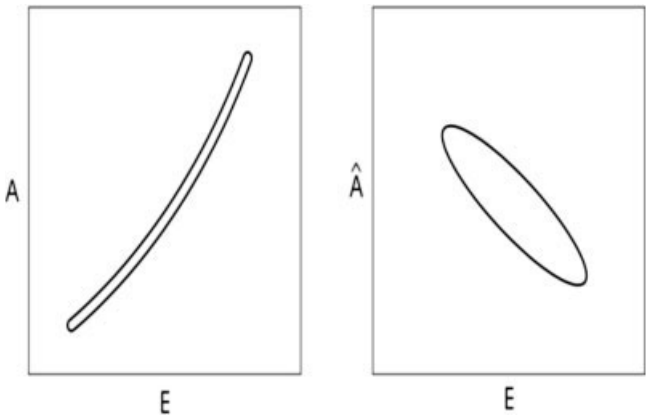

Figure 4 Parameter space transformation.

where M is the number of heating rate measurements. To overcome correlation among the model parameters, the functional minimization was replaced by the following expression

$$S(\boldsymbol{\Theta},\bar{\beta}) = S(\hat{\boldsymbol{\Theta}},\bar{\beta}) \cdot \left[1 + \frac{p}{n-p} F(p,n-p,\gamma)\right] \quad (12)$$

where $F(p,n-p,\gamma)$ is Fisher's F distribution with p and $n-p$ degrees of freedom (n is the number of observed responses, p is the number of unknown parameters, γ is the desired significance level), $S(\hat{\boldsymbol{\Theta}},\bar{\beta})$ is the minimum value of the objective function, and $\hat{\boldsymbol{\Theta}}$ is the parameter vector value in minimum. The preexponential factors (A_i) and activation energies (E_i) for a particular rate constant tend to be highly correlated.[11] From the computational point of view, this means the numerical solution of the problem of estimating Arrhenius parameters takes the form of a long ''narrow valley.'' To overcome this trouble, reparameterization, centering the temperature factor above a sensible reference value, $\hat{T}$ (in our case $\hat{T} = 300^{\circ}\mathrm{C}$), is suggested. An appropriate choice for $\hat{T}$ is the average temperature over the whole range of the experiments. The Arrhenius rate constant, $k(T)$, now is in a reformulated form:

$$\begin{aligned} k(T) &= A \cdot \exp\left(-\frac{E}{RT}\right) \\ &= \hat{A} \cdot \exp\left[-\frac{E}{R}\left(\frac{1}{T} - \frac{1}{\hat{T}}\right)\right] \\ \hat{A} &= A \cdot \exp\left(-\frac{E}{RT}\right) \end{aligned} \quad (13)$$

where $\hat{A}$ is the reformulated preexponential factor. The reformulation procedure with reshaped confidence region is illustrated by Figure 4.

The parameter estimation procedure can be conducted with a reformulated parameter space such as

$$\boldsymbol{\Theta} = \{\hat{A}_1, E_1, n, \lambda_1, \hat{A}_2, E_2, m, \lambda_2\} \quad (14)$$

The minimization of the objective function $S(\boldsymbol{\Theta},\bar{\beta})$ was carried out with the modified Nelder–Mead simplex search algorithm.[11] The ''elongated valley'' shape of the minimization function, common for chemical kinetics problems, needs an efficient search procedure. The set of fixed search parameters is replaced with flexible search parameters, where the expansion phase in the search direction is optimized.[12] In the minimization procedure nonnegativity constraints should be taken into account:

$$\begin{aligned} &\lambda_i \geq 0 \\ &A_i \geq 0 \qquad i = 1,2 \end{aligned} \quad (15)$$

Sometimes inaccurate models distort parameter values, and an additional ''penalty'' term needs to be introduced into the function:

$$\hat{S}(\boldsymbol{\Theta},\bar{\beta},\mu) = S(\boldsymbol{\Theta},\bar{\beta}) + \mu \cdot (1 - \lambda_1 - \lambda_2) \quad (16)$$

where μ is the penalty parameter. For PU elastomers based on a poly(ether polyol) soft segment and an aromatic type of diisocyanate, optimal parameter vectors are estimated.

Confidence regions are of primary importance because they provide a way to judge the accuracy of parameter estimates. Because the objective functional $S(\boldsymbol{\Theta},\bar{\beta})$ represents the closeness of the experimental data to the fitted model, basing the confidence region of Θ on the contours of $S(\boldsymbol{\Theta},\bar{\beta})$ is justified. In the parameter space, such a region has the general form

$$\left\{\boldsymbol{\Theta};\, S(\boldsymbol{\Theta},\bar{\beta}) \leq S(\hat{\boldsymbol{\Theta}},\bar{\beta}) \cdot \left[1 + \frac{p}{n-p} F(p,n-p,\gamma)\right]\right\} \quad (17)$$

The surface of the measure of goodness of fit gives some information about the reliability and clearly shows if the problem is not identifiable, but how to transform this information into confidence limits and how to visualize multidimensional surfaces are complicated tasks. Confidence regions in parameter space can be expressed in the quadratic form

$$\left\{\boldsymbol{\Theta};\, (\boldsymbol{\Theta} - \hat{\boldsymbol{\Theta}})^T \cdot C^{-1} \cdot (\boldsymbol{\Theta} - \hat{\boldsymbol{\Theta}}) \leq S(\hat{\boldsymbol{\Theta}}) \cdot \left[1 + \frac{p}{n-p} F(p,n-p,\gamma)\right]\right\} \quad (18)$$

where C is the parameter covariance matrix for the linear case. In the linear case contours defined by eq. (18) are ellipsoids in the Θ space centered at $\hat{\boldsymbol{\Theta}}$, whereas for nonlinear systems the shape of the γ-level contours can be distorted because of the nonlinearity of the relationship between parameters and model outputs. To estimate the parameter uncertainties with reliable extrapolation into nonmeasurable regions, the Monte Carlo simulation may be useful.[13] Optimal experiment design criteria require that the ''real'' parameters of a given system probably lie somewhere inside the confi-

TABLE I
Kinetic Parameters Determined by Optimization Procedure

	HS content (%)	SS molecular weight (g/mol)	A_1 (s^{-1})	E_1 (kJ/mol)	n	A_2 (s^{-1})	E_2 (kJ/mol)	m	λ
Sample 1	35	1000	6×10^7	118	1.2	5×10^{11}	185	1.02	0.42
Sample 3	35	2000	1.6×10^8	167	1.4	7×10^{12}	198	1.01	0.22
Sample 4	53	2000	1.8×10^8	130	1.15	4.5×10^{11}	183	1.08	0.3
Sample 2	52	1000	2.3×10^8	110	1.6	2.5×10^{12}	192	1.05	0.6
	45	1000	4×10^8	98	1.3	8×10^{11}	184	1.1	0.49
	44	2000	1.9×10^8	129	1.2	4×10^{12}	185	1.09	0.51

dence region. Confidence regions of the estimated parameters indicate their spread, the correlation with each other. For a nonlinear system, the shape of the confidence region may be heavily influenced by the curvature.

RESULTS AND DISCUSSION

For the samples with different structural parameters (HS content and SS molecular weight), the optimization procedure was applied, and components of the parameter vector at minimum, $\hat{\Theta}$, are listed in Table I. Thermogravimetric analysis was performed at heating rates of 2°C/min, 5°C/min, 10°C/min, and 15°C/min under a nitrogen gas flow. Figure 5 shows the TG and DTG (derivative thermogravimetry) curves for PU elastomer decomposition in nitrogen, as well as the best-fit overall conversion curves fitted by the reaction kinetic eq. (9). The degradation process was characterized by a kinetic ''triplet'' (activation energy, E_i; conversion function, f_i, with reaction orders n and m; and preexponential factor, A_i) measured with TGA experimental data. The kinetic parameters for each degradation stage were calculated by the Nelder–Mead optimization procedure at min, Θ, and by the Kissinger method,[14] and the results are summarized in Tables I and II, respectively. Generally speaking, because the mechanism (chemical-bond breakage) of thermal decomposition of PU changed during degradation, the activation energy was dependent on the HS and SS contents, as well as on the types of isocyanate and SS and the SS molecular weight. In our previous investigation in which we qualitatively characterized thermal degradation for the same PU elastomers, we concluded that PU elastomers based on poly(ester polyol) and aromatic diisocyanate exhibited better thermal stability than ether-based PU elastomers with the same molecular weight ($M_w = 1000$). Furthermore, the PU elastomers based on higher-molecular-weight poly (ether polyol) showed better thermal stability.[15]

- A_1, A_2—Preexponential factors of the first and second stages of degradation.
- E_1, E_2—Activation energies of the first and second stages of degradation.
- n, m—Reaction orders of the first and second stages of degradation.
- $\lambda_1 = \lambda$, $\lambda_2 = 1 - \lambda$—Yield coefficients.

Table I shows that the activation energy in the first degradation stage (E_1) decreased with an increase in HS content for the same SS content. This behavior was

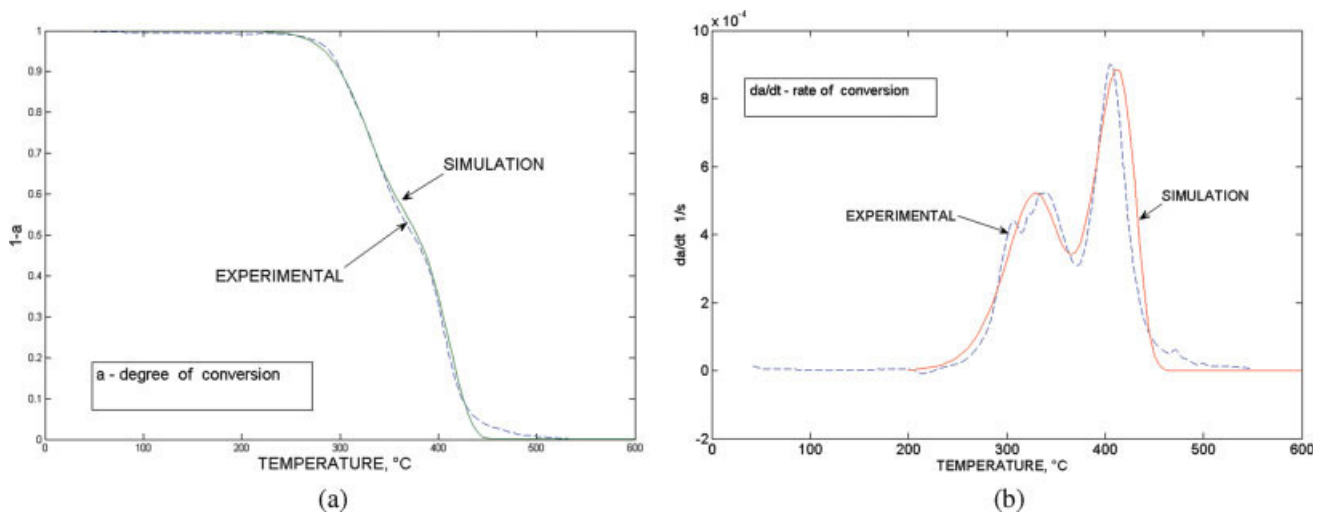

Figure 5 (a) TG experiment and curve fit model; (b) DTG experiment and curve fit model. [Color figure can be viewed in the online issue, which is available at www.interscience.wiley.com.]

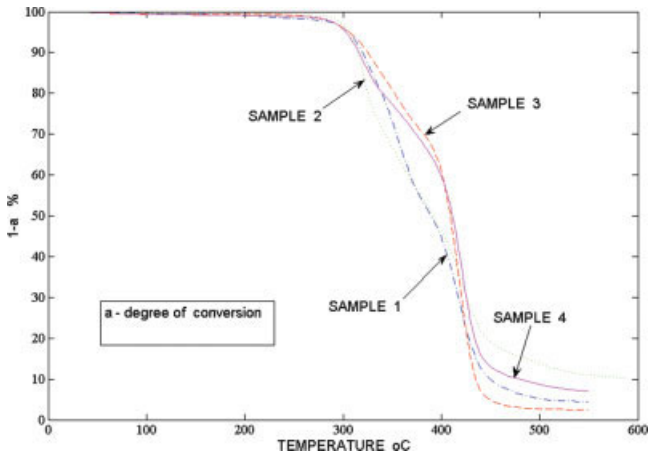

Figure 6 TGA thermograms at a heating rate of 5°C/min.

more pronounced in PU elastomers with a higher SS molecular weight ($M_w = 2000$). It is known that MDI has a chemical structure with a high degree of symmetry, which leads to a high degree of intermolecular hydrogen bonding. Thus, MDI has a high degree of hard-segment crystallinity.[15] A higher activation energy in the second degradation stage (E_2) was associated with higher thermal stability of the soft segment. Similar results for activation energy were seen with the Kissinger method (Table II). The TGA thermograms in Figure 6 indicate the samples' different behavior.

The overall reaction orders n and m were not fixed to 2 according to the theoretical consideration.[16] The DTG curve used for the objective function was superior to the TG curve for many reasons, one of which was that the DTG curve was more sensitive to perturbation.[8]

Figure 7 shows the experimental DTG profiles of three samples with the same heating rate ($\beta = 5°C/min$) but different HS contents (35%, 45%, and 52%). The HS content influenced the shape of the curve (shape index, inflection point, skewness).[18] The conversion function type directly influenced the quality of interpolation. It was rational to suppose that morphological descriptors of a hard-segment structure determined the type of conversion function. One possible reaction model adaptable to a wide range of polymers is the extended Prout–Tompkins model[19]:

$$f = [1 - C(1 - \alpha)]^n (1 - \alpha)^m \tag{19}$$

where C, n, and m are constants.

TABLE II
Activation Energies Calculated by Kissinger method[14]

HS content (%)	SS molecular weight	E_1 (kJ/mol)	E_2 (kJ/mol)
35	1000	118	185
35	2000	148	192
53	2000	130	193
52	1000	101	137
45	1000	92	149
44	2000	135	191

Response surface methodology

Calculated scatter data for the activation energy in the first and second stages of degradation (one component of the estimated parameter vector, Θ) are related to HS content and SS molecular weight. Using a response surface interpolation procedure,[20] a functional relationship between activation energy as the dependent variable and HS content as well as SS molecular weight as the independent variables was established:

$$\begin{aligned} E_1 &= E_1(c, M_w) \\ E_2 &= E_2(c, M_w) \end{aligned} \tag{20}$$

where c and M_w are HS content and SS molecular weight, respectively. The bilinear polynomial model was used for both the first and second degradation steps:

$$\begin{aligned} E_1 &= \beta_0 + \beta_1 x_1 + \beta_2 x_2 + \beta_{12} x_1 x_2 \\ E_2 &= \gamma_0 + \gamma_1 x_1 + \gamma_2 x_2 + \gamma_{12} x_1 x_2 \end{aligned} \tag{21}$$

where the dimensionless variables x_1 and x_2 are

$$\begin{aligned} x_1 &= \frac{c - \frac{1}{2}(c_{\min} + c_{\max})}{\frac{1}{2}(c_{\max} - c_{\min})} \\ x_2 &= \frac{M_w - \frac{1}{2}(M_{w\min} + M_{w\max})}{\frac{1}{2}(M_{w\max} - M_{w\min})} \end{aligned} \tag{22}$$

The constants β_{ij} and γ_{kl} were determined by multiple regression analysis using data from Table I, with the values $\beta_0 = 126$;, $\beta_1 = -12.18$, $\beta_2 = 17.1$, $\beta_2 = 17.1$,

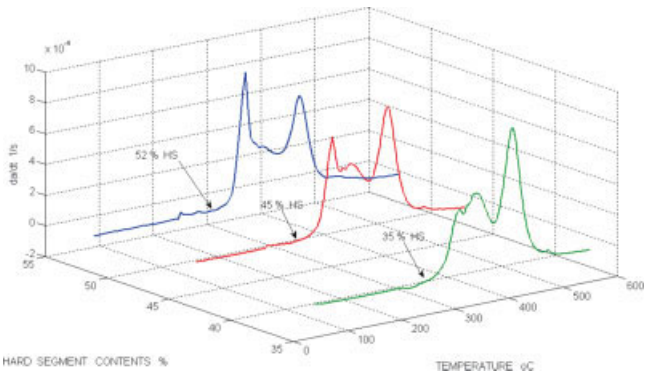

Figure 7 DTG profiles of different HS contents. [Color figure can be viewed in the online issue, which is available at www.interscience.wiley.com.]

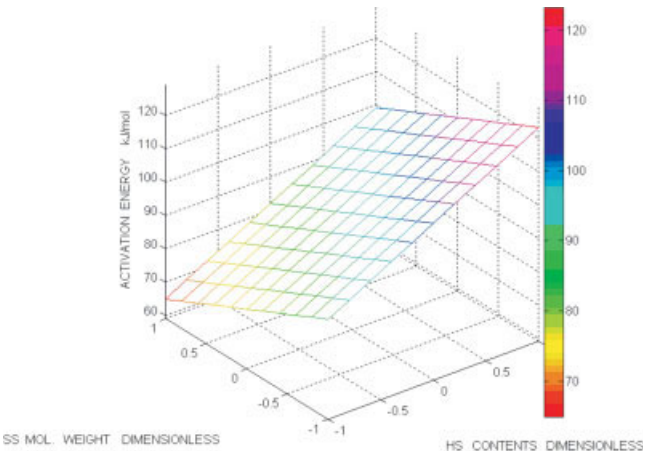

Figure 8 Dependence of activation energy, E_1, on HS content and SS molecular weight (first stage). [Color figure can be viewed in the online issue, which is available at www.interscience.wiley.com.]

$\beta_{12} = -7.28$, $\gamma_0 = 186$, $\gamma_1 = -2.04$, $\gamma_2 = 0.65$, and $\gamma_{12} = -2.56$.

The independent variable c ranged from 34% to 54% and the independent variable M_w ranged from 1000 to 2000 g/mol. Figure 8 shows the isolevel curves for the average activation energy of the PU elastomers in the first stage of degradation. According to the results, the activation energy of the PU elastomers increased as the soft-segment molecular weight increased. The activation energy of the PU elastomers decreased as the HS content increased. The gradient of the activation energy of the first stage of degradation suggests that the HS content had a significant effect on the type of conversion function of the thermal degradation processes. The data on the dependence of HS content as well as SS molecular weight on the activation energy of the second stage of degradation are shown in Figure 9, suggesting that activation energy was not dependent on HS content.

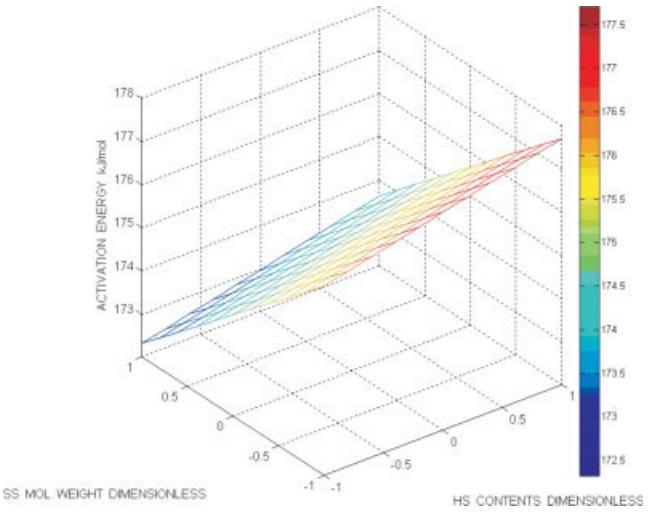

Figure 9 Dependence of activation energy, E_2, on HS content and SS molecular weight (second stage). [Color figure can be viewed in the online issue, which is available at www.interscience.wiley.com.]

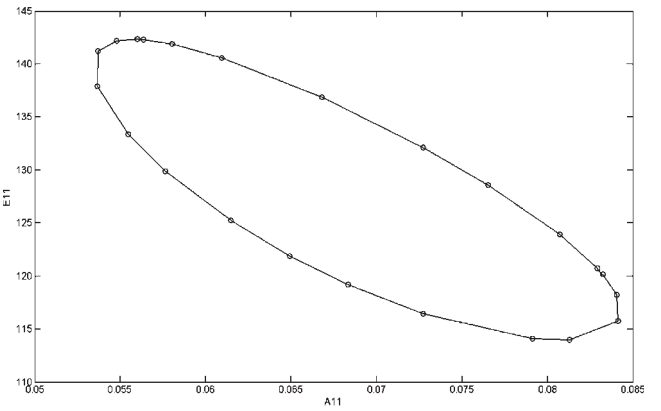

Figure 10 Confidence region, $\hat{A}_{11} - E_1$, for the first step of the degradation.

A plane with orthogonal parameter axes was formed by wearing two parameters and holding the other constant at its optimal $\hat{\Theta}$. The activation energy and corresponding preexponential factor were wearing parameters. The contour plots of the 95% confidence region for the sum-of-squared-errors surface are shown in Figures 10 and 11. Figure 10 shows the plot of the confidence region for the first degradation stage, $\hat{A}_1 - E_1$, whereas Figure 11 shows the plot of the confidence region for the second step, $\hat{A}_2 - E_2$. This region is exact because it was not based on any approximation. The system was more sensitive to activation energy changes then to preexponential factors. The second step was more nonlinear (contour is far from ellipse), and the confidence limit was narrower, heavily influenced by the curvature.

CONCLUSIONS

For PU elastomers based on a poly(ether polyol) soft segment and an aromatic type of diisocyanate,

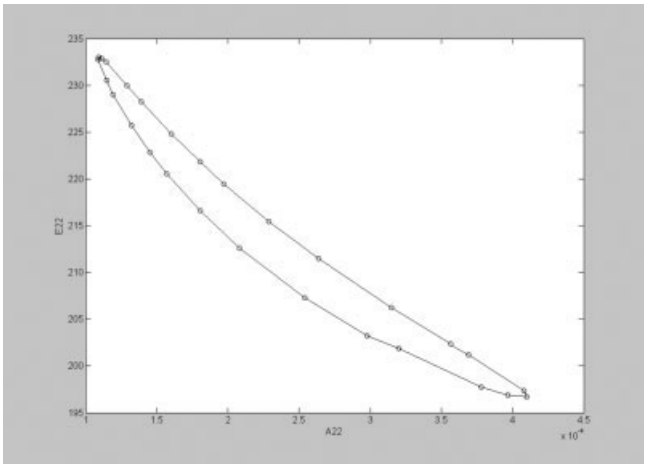

Figure 11 Confidence region, $\hat{A}_{22} - E_2$, for the second step of the degradation.

the optimal parameter vector was estimated with associated confidence interval using a nonlinear regression procedure. The DTG curve followed a two-step decomposition process with high-level sensitivity to uncertainty. Therefore the DTG curve was chosen for the objective function. The first stage of decomposition was correlated with HS degradation, whereas the second peak correlated with the degradation of the SS. In the present work it was observed that PU elastomers with a higher hard-segment content and a higher soft-segment molecular weight exhibited higher thermal stability. The E_1 of the PU elastomers was highest with a higher soft-segment molecular weight. Increasing the soft-segment molecular weight decreased the compatibility of the hard and soft segments and hence increased phase separation. The higher degree of hard-segment crystallinity and phase separation may have been why PU elastomers that had higher-molecular-weight soft segments ($M_w = 2000$) had better thermal stability and higher activation energy. The resulting fitting of the second stage of degradation was more or less successful for all samples. A discrepancy between the experimental and simulation data was evident in the first stage of degradation. More precisely describing the morphology of the hard-segment structure may be another way to make a better choice of conversion function.

References

1. Cunningham, A. R. M.Sc. Thesis, Massachusetts Institute of Technology, Cambridge, MA, 1997.
2. Hepburn, C. Polyurethane Elastomers, 2nd ed.; Elsevier: Amsterdam, 1991.
3. Duquesne, S.; Le Bras, M.; Bourbigot, S.; Delobel, R.; Camino, G.; Eling, B. Polym Degrad Stabil 2001, 74, 493.
4. Lee, H. K.; Ko, S. J Appl Polym Sci 1993, 50, 1269.
5. Day, M.; Corney, J. D.; MacKinnon, M. Polym Degrad Stabil 1995, 48, 341.
6. Malec, E. J.; David, D. J.; Staley, H. B., Eds. Analytical Chemistry of Polyurethane; Wiley & Sons: New York, 1969.
7. Agić, A.; Govorčin Bajsić E.; Rek, V. J Elastomers Plastics 2006, 38, 105.
8. Mamleev, V.; Bourbigot, S.; Bras, M.; Duquesne, S.; Šestak, J. Phys Chem Chem Phys 2000, 2, 4796.
9. Lyon, R. E. Thermochimica Acta 1997, 297, 117.
10. Sempere, J.; Nomen, R.; Serra, R.; Soravilla, J. Thermochim Acta 2002, 388, 407.
11. Himmelblau, D. M. Process Analysis by Statistical Methods; Wiley & Sons: New York, 1970.
12. Marsili-Libelli, S.; Castelli, M. Appl Math Computation 1987, 23, 341.
13. Hessler, J. P. Int J Chem Kinet 1997, 29, 803.
14. Kissinger, H. E. Anal Chem 1957, 29, 1702.
15. Bajsic, E. G.; Rek, V. J Appl Polym Sci 2001, 79, 864.
16. Song, Y. M.; Chen, W. C.; Yu, T. L.; Lin, K.; Tseng, Y. H. J Appl Polym Sci 996, 62, 827.
17. Kim, D. S.; Kim, J. T.; Woo, W. B. J Appl Polym Sci 2005, 96, 1641.
18. Chang, W. I. J Appl Polym Sci 1994, 53, 1759.
19. Burnhan, A. K.; Weese, R. K. Lawrence Livermore National Lab. UCRL-CONF-203168, 2004.
20. Myers, R. H.; Montgomery, D. C. Response Surface Methodology; Wiley Interscience: New York, 1995.
21. Petrović, Z. S.; Zavargo, Z.; Flynn, J. H.; Macknight, W. J. J Appl Polym Sci 1994, 51, 1087.